Robotica (2000) volume 18, pp. 263–272. Printed in the United Kingdom © 2000 Cambridge University Press

Draper unmanned vehicle systems

David S. Kang, Jamie M. Anderson and Paul A. DeBitetto

Draper Laboratory, 555 Technology Square, Cambridge, MA 02139 (USA)

SUMMARY

Draper Small Autonomous Aerial Vehicle (DSAAV), MITy and SMART micro-rovers, Companion mini-rover, and Vorticity Control Unmanned Undersea Vehicle (VCUUV) are highlighted. DSAAV demonstrated autonomy with GPS/INS integration and vision processing. The micro- and mini-rovers investigated ground based autonomy with extensive mapping and planning integration. VCUUV is a flexible-hull UUV which propels and maneuvers like a tuna.

KEYWORDS: Autonomous mobile robots; Telerobotics; Rovers.

1. INTRODUCTION

The unmanned systems highlighted are developed in the Intelligent Unmanned Vehicle Center of Draper Laboratory. The center represents a cooperation with Draper Laboratory and universities in the Boston area (MIT, Tufts, Boston Univ., Northeastern Univ.) to actively foster innovative research and design of intelligent systems. This paper presents a brief description of a collection of the vehicles developed or under development in the center.

2. AERIAL VEHICLE

The Draper Small Autonomous Aerial Vehicle (DSAAV) (Figure 1) is a prototype of a complete mini-helicopter UAV system that includes a small helicopter, a lap-top ground station, a video down link and an optional ground vision processing work station. The goal was to develop a small yet capable research platform that would be used to develop and demonstrate autonomous capabilities.

The DSAAV currently consists of Draper-developed avionics residing on a Bergen industrial R/C helicopter platform. The heart of DSAAV's navigation hardware is an integrated INS/GPS system, which combines the accuracy and stability of a DGPS receiver with the high bandwidth and the self-contained nature of inertial navigation. Since DSAAV makes autonomous landings, a sonar altimeter is needed to accurately detect the location of the ground below the vehicle. Finally, DSAAV is equipped with a digital compass to compensate for IMU heading drift.

Six servos provide control actuation to DSAAV's control surfaces and throttle. Control commands are issued either by the safety pilot's R/C transmitter or the on-board control system. The receiver interface translates these commands and sends them to the vehicle's servos. Guidance, navigation, control, and communication data are processed in the on-board computer, which consists of a 100 MHz 486 processing board, an ethernet board, and an I/O board. The processor runs the QNX operating system, which is a UNIX-like real-time operating system. DSAAV's on-board computer and the other electronics are powered by a NiMH battery pack, which powers the equipment for about 60 minutes.

The initial design was based largely on the requirements for the 1996 International Aerial Robotics Competition, sponsored by the Association for Unmanned Vehicle Systems International, AUVSI. The competition occurs on a 60 by 120 ft. field with five randomly placed and randomly oriented 55-gallon drums. The DSAAV took first place, being the first to perform the contest mission fully autonomously from take-off to landing. The DSAAV system flown in the competition can be flown for approximately 25 min with the stock fuel supply. Its top speed under manual control is approximately 70 mph.

The DSAAV system is currently validated for autonomous flight at around 20 ft/sec, takeoffs, hovering, pilot assist flight, and landing. Figure 2 is a functional block diagram. The box delineates the on-board system from the ground system.

The vehicle can be flown in a full range of autonomous guidance modes: ground mode, runup mode, takeoff mode,

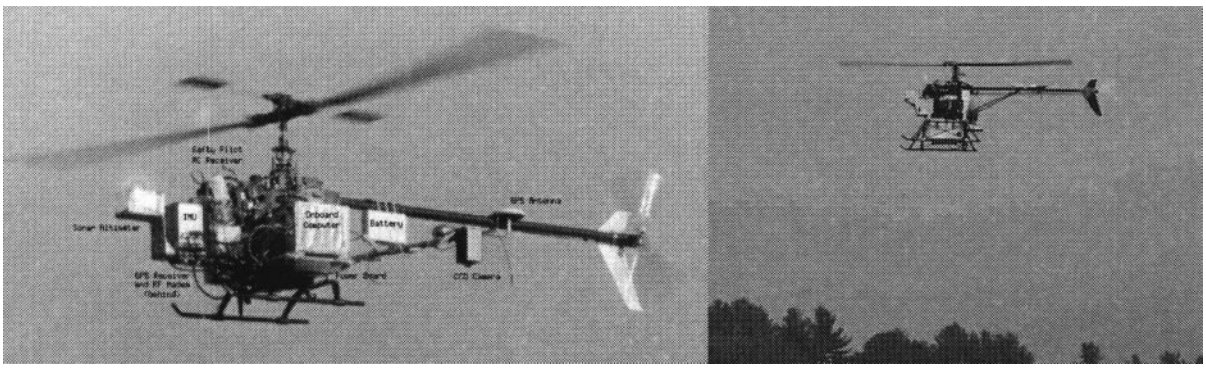


Fig. 1. Draper small autonomous aerial vehicles.

https://doi.org/10.1017/S0263574799002246 Published online by Cambridge University Press

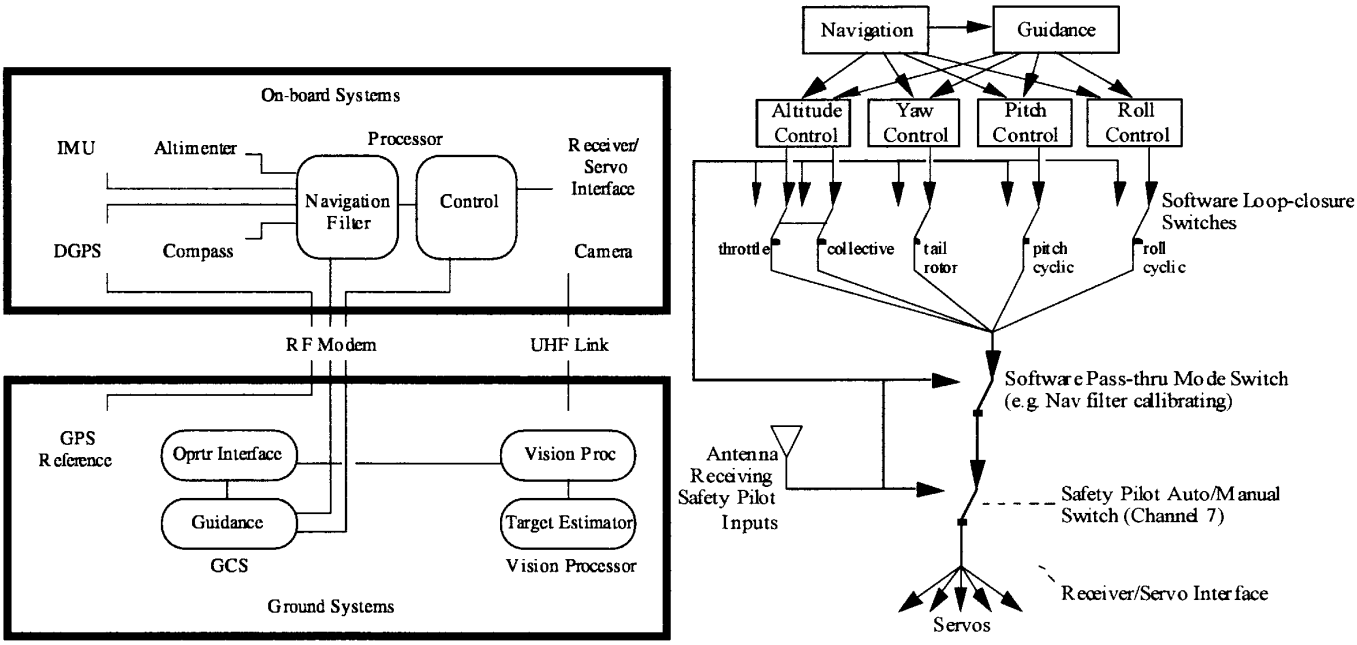


Fig. 2. Functional block diagram.

waypoint hover mode, waypoint through mode, track hover mode, track through mode, waypoint land mode, and pilot assist mode.[1]

Ground mode is the guidance mode the helicopter is in when it is sitting on the ground, not executing a mission. In ground mode, the guidance algorithm commands a very low throttle setting, so the engine will idle and the operator can safely approach the vehicle, if necessary. In runup mode, the engine throttle is gradually ramped up to its takeoff level. The pitch of the main rotors blades, however, remains zero so that they produce no lift. Runup mode allows the engine to achieve takeoff RPMs without actually committing the vehicle to a takeoff maneuver.

In takeoff mode, the computer continues commanding the runup throttle setting, while the collective pitch of the main rotors is gradually increased, creating enough lift to pick the DSAAV off the ground and take it to the takeoff altitude. When the vehicle is on or near the ground, the guidance algorithm makes no attempt to command a horizontal position for the helicopter. If any part of the vehicle is still in contact with the ground, any command to correct for a horizontal position error could cause the helicopter to roll over on the ground.

In waypoint hover mode, the guidance algorithm commands the helicopter to a specified location and altitude for a specified hover time. The waypoint hover mode commands the most direct trajectory between the DSAAV's present position and the commanded hover position. In waypoint through mode, the helicopter does not stop and hover at the waypoint, rather it merely passes through the waypoint location on its way to the next waypoint. The waypoint land mode is broken up into several submodes. First, the guidance algorithm commands the helicopter to hover above the landing location. Once there, the DSAAV descends to the "landing altitude", which is its last stop on the way to the ground. Currently this landing altitude is 3 feet. The vehicle hovers at the landing altitude until the vertical and horizontal velocities are small enough (~0.5 feet/sec) for a safe landing, and then begins descending at a constant rate of 0.5 feet per second.

When the DSAAV is 1.5 feet from the ground, the guidance algorithm begins ramping the collective and throttle commands from their hover values down to their ground mode values. Decreasing the collective and throttle commands causes the helicopter to do a fairly rapid controlled descent for those final few inches until it reaches the ground. This final stage of the landing maneuver is open loop; the software does not try to eliminate position and velocity errors. Doing so would increase the chance of a rollover on touchdown.

Track hover and track through modes are the same as waypoint hover and waypoint through mode, except the vehicle is commanded to follow a straight-line ground track between successive waypoints. If the helicopter drifts off the track on its way to the waypoint, the control system commands it back on the track.

Pilot assist mode allows the GCU operator to directly command the vehicle's position/altitude/heading with the joystick, while the inner-loop control system maintains stability. Once the operator releases the joystick, the DSAAV continues hovering at its present location. Pilot assist is a quick, intuitive way for the operator to accurately position the helicopter. It is especially useful when finding and viewing objects from the DSAAV's on-board camera. Given the current guidance mode, the guidance algorithm will output the appropriate position, velocity, and attitude commands to the control code.

For the competition, a grey-scale CCD camera with a UHF transmitter was mounted on the helicopter and faced downward so the drum labels would be visible. The video images from the camera are buffered until they are matched to corresponding vehicle state information from the on-board navigation system. The state vector is used to transform image coordinates into drum positions relative to

https://doi.org/10.1017/S0263574799002246 Published online by Cambridge University Press

the contest field. The drum detector has three parts: a gradient operator, a matched filter, and a peak extractor. Figure 3 illustrates the image of a typical scene viewed from 10 feet above the barrels, the gradient image for the scene, and the output of the matched filter. During the winning flight, all five drums were located and two classified correctly.[2] The current vision system on board the DSAAV consists of a small, color CCD camera and a UHF transmitter, which transmits live video to the ground. The operator can adjust the tilt and zoom of the camera from the ground.

The DSAAV provides a valuable testbed for autonomous systems development, especially autonomous control algorithms. Development of DSAAV's hierarchical control system was facilitated by algorithm testing in simulation and actual vehicle flight tests. Draper and MIT continue GNC research using the DSAAV as a testbed.

3. GROUND VEHICLES

3.1 Micro-rovers

MITy. The micro-rovers are small – typically under a meter in length, – lightweight, and cost effective when compared to more traditional, larger vehicles. The rovers are equipped with a six-wheel drive flexible frame, front and rear Ackerman steering mechanisms and a modular chassis. The flexible frame provides a high degree of maneuverability, enabling the rover to traverse rocks, curbs, and uneven terrain. MITy-1, Figure 4, is based on a 2 MHz M68HC11 microcontroller. MITy-1 uses a magnetic compass and a drag wheel to determine heading and position. A sonar range finding module, switch-actuating feelers, and bumpers are used for hazard detection and obstacle avoidance.

The MITy-2, Figure 5, is based on 12 MHz Zilog processor. Navigation sensors include a gyroscope and a custom built sun sensor, tachometers, and an optical drag wheel. Obstacle avoidance is accomplished through the use of a scanning laser range finder, angular sensors to measure the vehicle pitch and roll, and two forward-looking optical proximity sensors for detecting ledges.[3]

The control systems developed for the MITy-1 and MITy-2 micro-rover prototypes successfully performed the goal of autonomous navigation in unknown environments.[4]

For MITy-1, the avoidance routines are only local in range to only avoid necessary obstacles. The MITy-2 path planner offers unified obstacle avoidance and target acquirement, allowing a longer range for planning that avoids trap situations and explicitly considers size and steering constraints of the rover. The efficiency of this routine allows reactive in-motion path planning and execution which rapidly incorporates new hazard and position information from sensors and ground control. The subgoal method of MITy-1 and the kinematic cost method of MITy-2 offer superior performance to attempted fuzzy logic and potential field methods, with regard to planning range and accuracy achieved with the prototype platforms.

In Monte-Carlo simulations, which subjected the rovers to 50 yard runs, 6 inches/sec, through random obstacle fields 100 times each, MITy-1 and MITy-2 reached their destinations 90% and 100% of the time respectively, with 10″ radius obstacles in a 6% distribution by ground coverage. The average path length to completion was 140% and 130% of the straight-line distance respectively for MITy-I and MITy-2. A plot of MITy-2's own position estimate while traversing a square path is shown in Figure 6. Note that the paths are not parallel to the square edges because of the minimum turn radius, but the end points are on the vertices. The actual mean position error was 4.45% with respect to nominal path distance. In comparison, field tests of MITy-1 showed the degree of successive error buildup. The average position error was 17.5% of the nominal path distance, which largely reflects compass problems.

In field tests, on average, MITy-1 is able to track its position within 5–7% for simple paths and few disturbances,

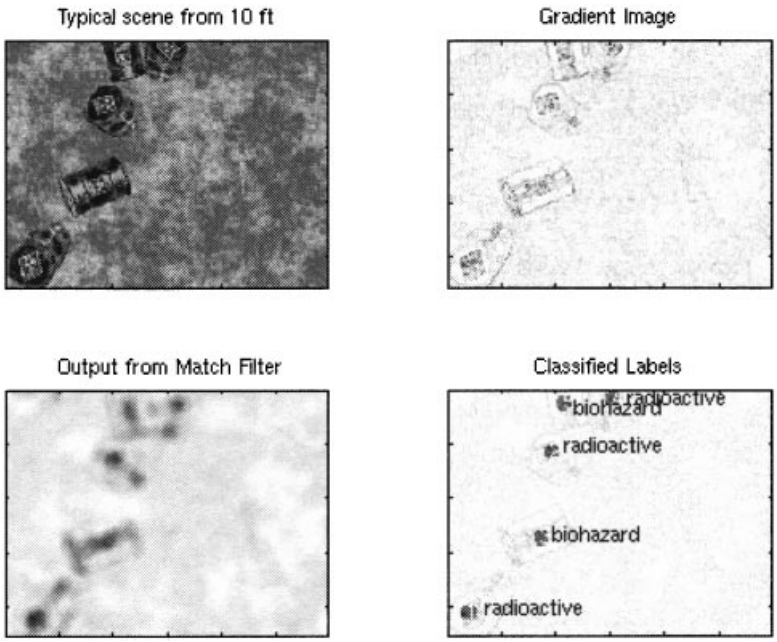


Fig. 3. Vision processing and label classification.

https://doi.org/10.1017/S0263574799002246 Published online by Cambridge University Press

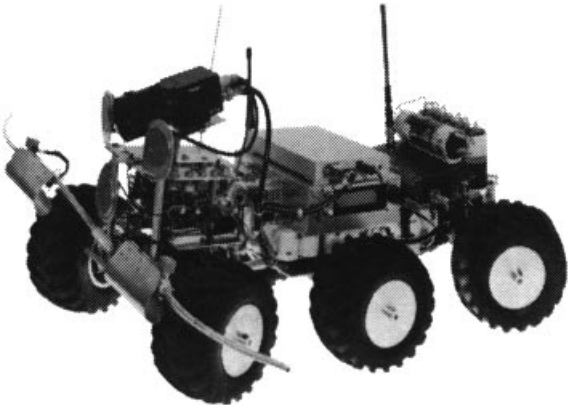


Fig. 4. MITy-1 micro-rover.

and 10-15% for more complex paths and maneuvers. In comparison, position tracking for MITy-2 came within 1% for simple cases and 4.5% for complex ones. These results reflect outdoor navigation over a variety of surfaces and sensor operating conditions. MITy-1 has repeatedly navigated obstacle fields with an average obstacle separation of 60 inches, in consideration of its 18 inch$\times$24 inch dimensions and 25 inch minimum turning radius, with few or no collisions. MITy-1 also consistently penetrated a 48 inch gap in a wail of obstacles with the same control parameter settings, indicative of its ability to reach a target as well as avoid obstacles.

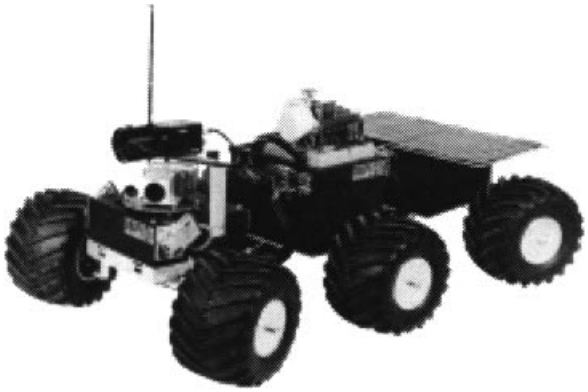


Fig. 5. MITy-2 micro-rover.

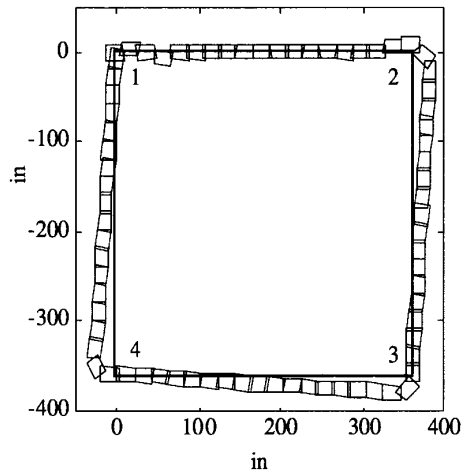


Fig. 6. MITy-2 square following.

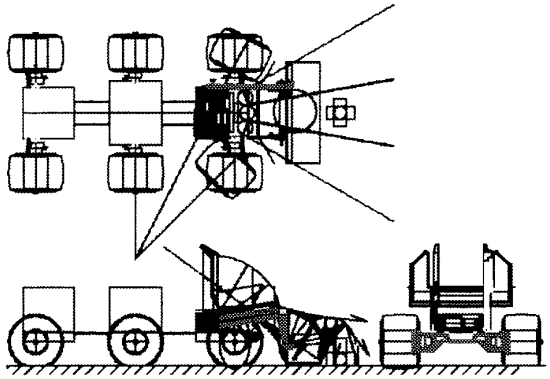


Fig. 7. SMART micro-rover.

SMART. The MITy prototypes are the predecessors for the current SMART (Small Autonomous Robotic Technician) system micro-rovers, Figure 7. These vehicles navigate to areas of indicated unexploded ordnance (UXO), locate them, pick them up, and carry them away to an ordnance disposal area (ODA). For buried mines, a charge is to be placed.

It is assumed that the approximate locations of the UXO within the area of operation are known *a priori*, but that the terrain conditions are not. Continuous update to the control station allows for the real-time construction of a map of the mission area.[5] The control station uses the A* search algorithm to plan the most efficient path to that location, given the initial obstacle information. An example solution of an A* search using an occupancy map is shown in Figure 8 with obstacles mapped in the mission area. The environment is broken up into known empty, known occupied, and unknown (yet to be mapped) regions. The planning problem is to provide the shortest obstacle-free path from the start node, S, to the goal node, X., minimizing exposure to unknown areas when known empty areas are not available.

The current research investigates remotely operated control interface suitable for controlling a micro-rover at high speed.[6] To overcome the sensor and processor limitations at high-speed travel, the operator station assumes availability of an overhead image. Based on this static image, a virtual rover path is overlaid using telemetry from the actual rover, Figure 9. Clockwise, the windows consist of Navigation, Video (rover level), Zoom (of Navigation window), Acoustic sensor range, Voltage, Velocity, and Buttons.

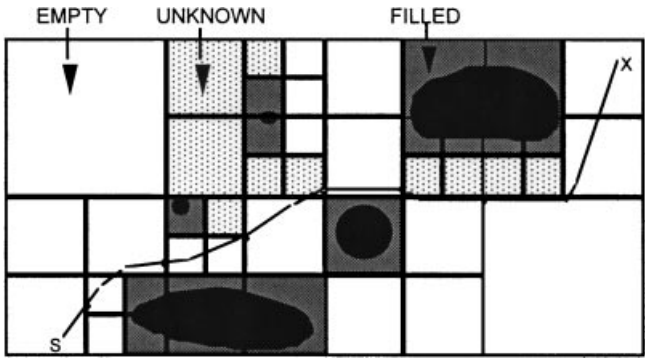


Fig. 8. Route planning using the A* search algorithm.

https://doi.org/10.1017/S0263574799002246 Published online by Cambridge University Press

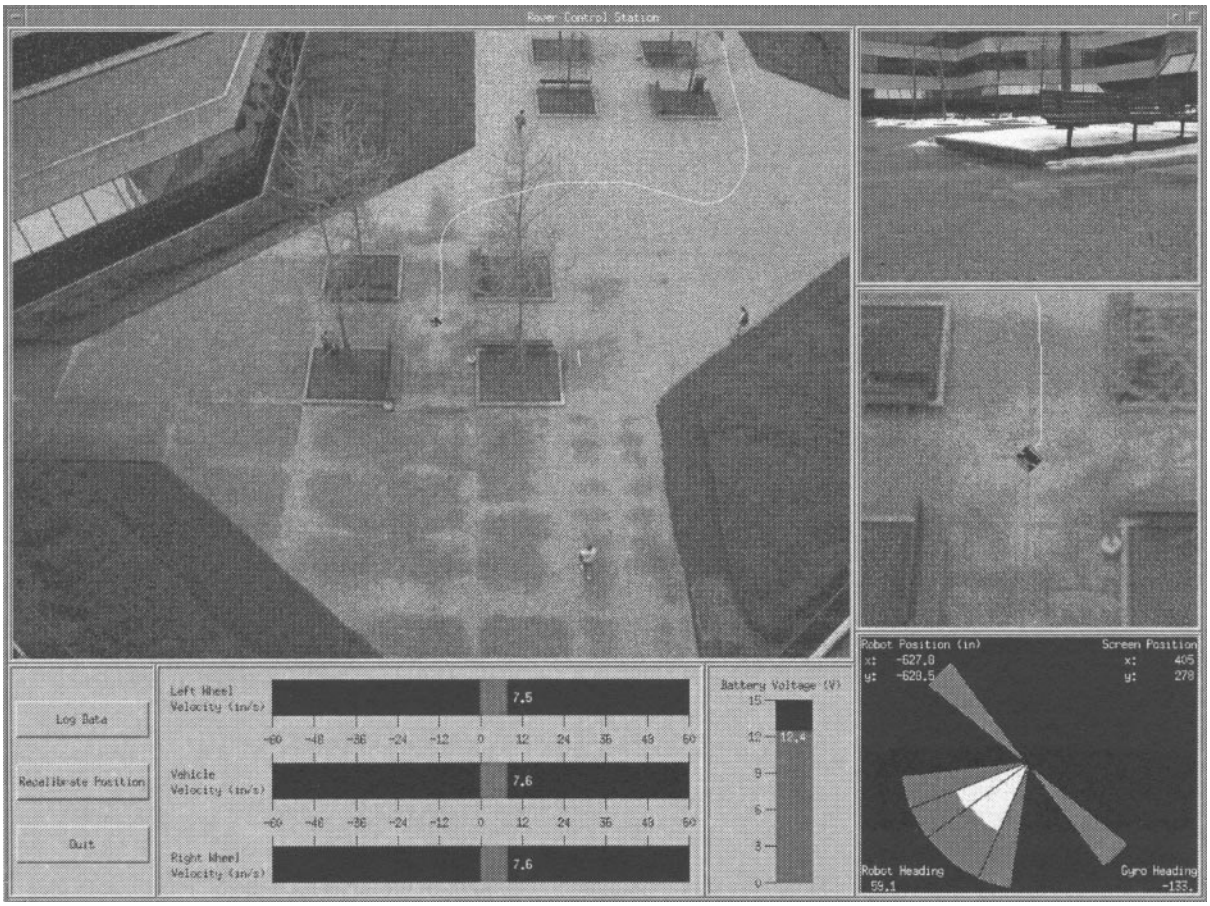


Fig. 9. Operator Control Station.

3.2. Mini-rover

Companion, Figure 10, is a 4-wheeled electric drive system with automobile-type steering, and an array of mapping and navigation sensors including a dual-axis scanning laser, sonar ring, and inertial sensors. It was designed as a generic test bed for autonomous mobile robot capabilities.[7] The specifications for the platform are shown in Table I. The dead reckoning sensors on Companion consist of heading and translation sensors. Heading is determined by an inertial angular rate sensor ("gyro") and a fluxgate magnetometer (electronic compass). Translation is measured with two optical quadrature encoders mounted to each of the front two wheels. In addition, the front wheel steering angles are measured with potentiometers.

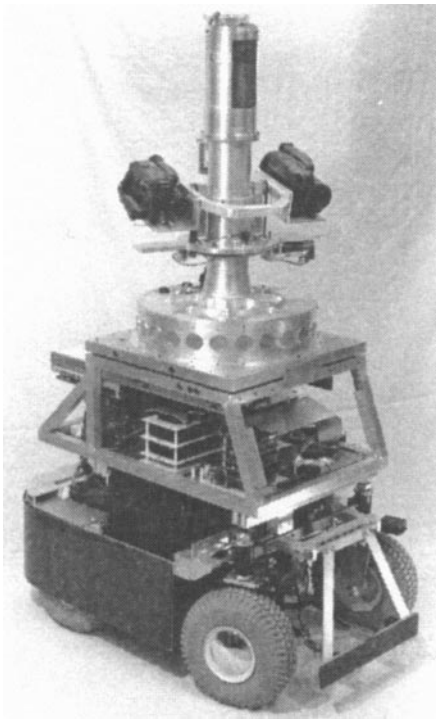


Fig. 10. "Companion" Robot (5 feet tall).

The Acuity laser range finder projects a beam of light at 780 nm (near infrared) from a laser diode. The mechanical scanner allows laser beam positioning of 360° in azimuth, and 90° in elevation. Companion's sonars, emit a variable

Table I: Mobility platform specifications

Specification	Value
full speed	5.5 mph
range	20 miles per charge
weight w/ batteries	200 lb
max load capacity	450 lb
climbing capacity	25°
wheel base	20 in.
turning radius	27 in.

https://doi.org/10.1017/S0263574799002246 Published online by Cambridge University Press

frequency "chirp" of about 50 kHz, resulting in a wavelength of a about $\frac{1}{4}$ inch. The sonar system has a maximum range of 36 feet, a range resolution of 1.7 inches (limited by the timer circuit), and a firing rate of 10 Hz. Companion uses an array of eight proximity switches in the front and rear and bumpers along the lower perimeter of the mobility platform. Companion's main processing is performed by two networked 486 computers. The two computers are networked by Ethernet, and both are running the QNX operating system.

In testing of Companion's dead reckoning, the distance of the robot's position as computed by dead reckoning from the actual position of the robot fell within 1% of the distance traveled during the test. Figure 11 shows two representative test runs conducted on a flat surface. In the top plot, the robot traveled forward 216 meters while making several turns along the way. In the bottom plot, the robot moved only 18 meters but was required to execute tight turns and changes in forward/reverse motion.

Mapping module implemented is a variation of an occupancy grid. The extensions added to the Companion implementation include the ability to dynamically grow the map, a hierarchical map structure, and the use of delayed evaluation for the certainty value. Blocks representing 1.5×1.5 square meter areas are dynamically added as needed. Under each of these blocks is a two level hierarchy where individual cells represent 15×15 square centimeter and 1.5×1.5 square centimeter areas. The lowest level in the hierarchy is only maintained near the robot. Thus the high resolution lowest level provides a local map. The medium resolution cells provide a global map.

The use of delayed evaluation for determining the certainty value (probability of an obstacle occupying a given grid element) greatly increases the flexibility of the system. This allows multiple search engines to interpret the state of the map differently. One possible extension this allows is for a search process to ignore a particular sensor.

Figure 12 shows a map generated by the robot's Mapper module in an indoor setting with straight walls and several openings. Dark marks in the map are 15×5 square centimeter regions whose probability of being obstructed are above a certain threshold. Testing to date has focused on the lower software modules of navigation and mapping. These have shown very good performance, and have laid the foundation for the remaining work in higher level planning and ground control station development. Although the robot is developed to be capable of full autonomy, it is recognized that successful operation will make variable use of the human operator as a supervisory controller, making realistic missions in unstructured environments possible.

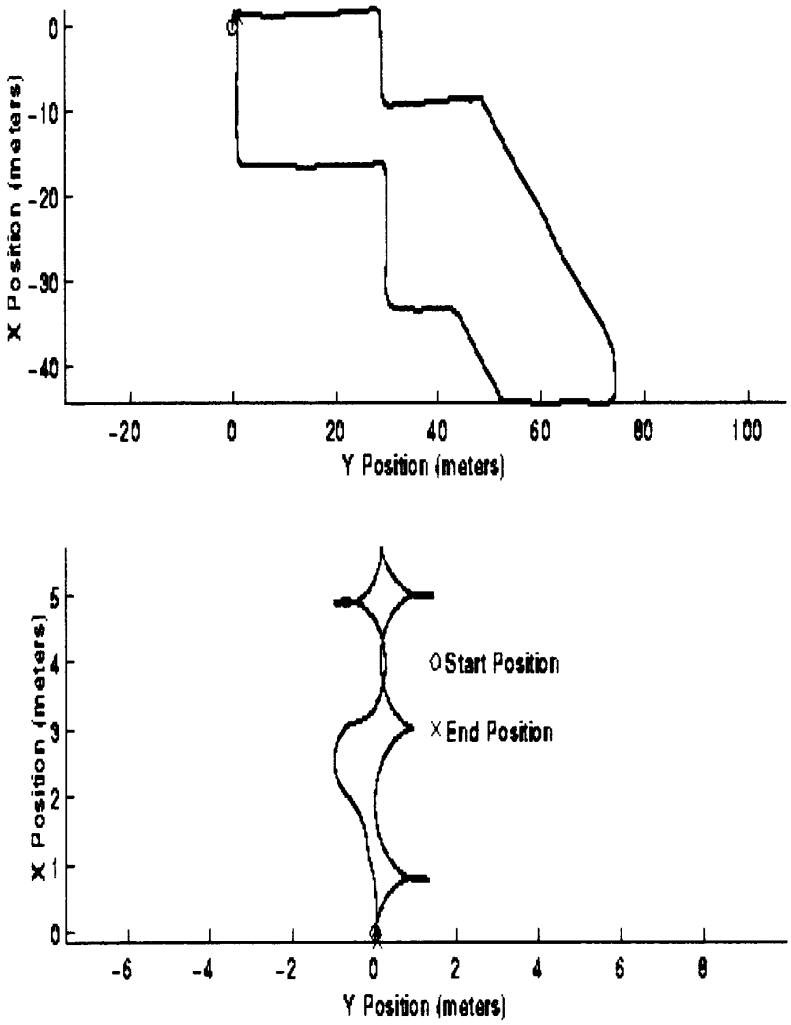


Fig. 11. Navigation Tests.

https://doi.org/10.1017/S0263574799002246 Published online by Cambridge University Press

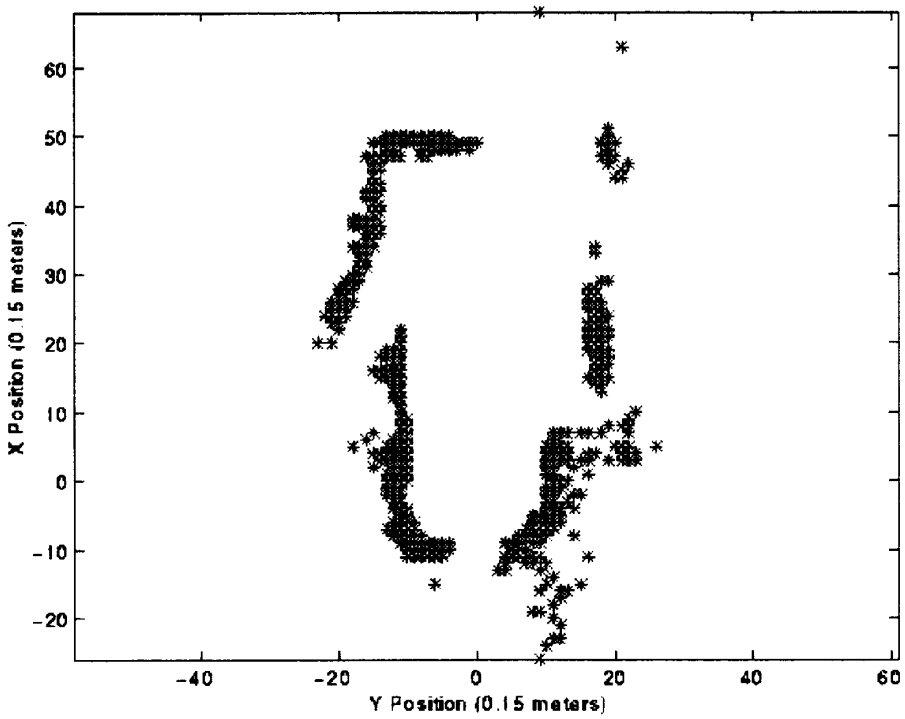


Fig. 12. Mapper test.

4. UNDERSEA VEHICLE

In recent years, research in the propulsion and maneuvering mechanisms used by fish has demonstrated the utility of bio-propulsion for undersea vehicles. Despite advances in unmanned undersea vehicle (UUV) technology, little progress has been made in improving propulsive efficiency and maneuverability. Most underwater vehicle designs employ a conventional propeller as the main propulsor and shrouded thrusters and/or control fins for maneuvering. Two types of vehicle designs are prevalent: torpedo shaped bodies streamlined for speed and range, or box-shaped bodies designed for maneuvering and station keeping. Unfortunately, most UUV missions require all of these capabilities: high transit speed, long range/duration, maneuverability and station keeping ability. Thus a fish is a potentially optimal UUV design in that they are able to cruise great distances at significant speed, maneuver in tight spaces and accelerate and decelerate quickly. As Figure 13 illustrates, this performance comes at moderate cost to vehicle displacement.

Draper Laboratory has developed and fielded the first biomimetic autonomous underwater vehicle which is sized appropriately for actual underwater missions. Named after the vorticity control flow control mechanisms employed by fishes to propel and maneuver, the Vorticity Control UUV (VCUUV), Figure 14, mimics the form and kinematics of a yellowfin tuna. Across the broad spectrum of fish form and movement, tunas are most desirable as a vehicle platform as they are very streamlined, relatively rigid in the forebody and propel with low amplitude movements in conjunction with a high performance hydrofoil (caudal fin). Most tunas swim continuously at one to two body lengths per second but can burst to speeds in excess of ten lengths per second. Additionally, tunas are highly maneuverable compared to conventional underwater vehicle systems, due largely to the

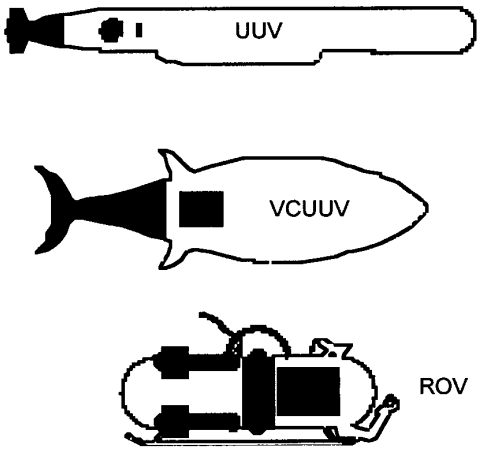


Fig. 13. Underwater vehicle comparison. The shaded portion of each vehicle indicates the propulson and maneuvering plant displacement. UUV (without cross axis thrusters) 4.5%, VCUUV 25%, ROV 50%.

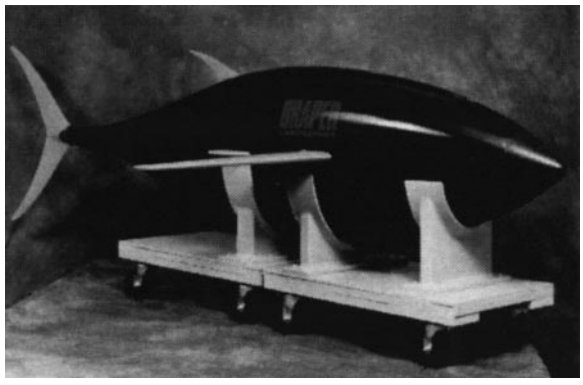


Fig. 14. Vorticity Control Unmanned Undersea Vehicle (VCUUV).

https://doi.org/10.1017/S0263574799002246 Published online by Cambridge University Press

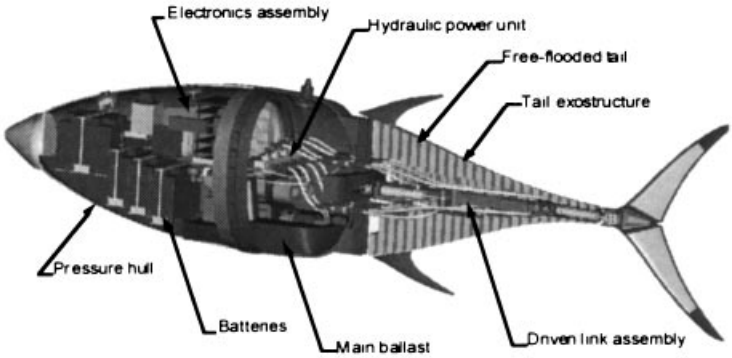


Fig. 15. VCUUV system diagram.

integrated nature of the main propulsor and maneuvering control surfaces. A tuna can execute a turn in less than its body length whereas typical torpedo shaped UUVs require several lengths to maneuver.

The primary goal of the VCUUV project was to produce an engineering proof of concept vehicle that could operate as a research platform to study the merits of flexible hull vehicles and the energetic costs of swimming and maneuvering like a fish. To meet these goals, the vehicle requirements were defined as follows:

Mechanical system:

- Fully autonomous operation
- Independent control of profile (phase and amplitude of each tail link element) at variable frequencies and vehicle speeds
- Near neutral buoyancy in articulated tail
- Minimum speed of 2.5 knots
- 2 body length turning diameter
- Minimum mission duration of 3 hours
- Missions in depths less than 10 *m*

Sensors:

- Measurement of vehicle location and orientation as a function of input kinematics
- Measurement of propulsive power (linkage velocity and force)
- Measurement of tail linkage position

Control:

- Closed loop control of tail linkage position
- Stable depth and heading

Figures 14 and 15 show the resulting VCUUV prototype and major systems and Table II summarizes the vehicle characteristics. The vehicle is 8 feet (2.4 *m*) long and has a dry weight of 313 lb (1392 N), and an envelope displacement of 371 lb (1650 N). The forward half of the vehicle comprises a pressure hull containing batteries, electronics (computers, sensors, etc.), the hydraulic power unit and payload. The pressure hull accounts for 73% of the vehicle envelope displacement. The design issues in the vehicle development are provided in detail by Anderson and Kerrebrock.[8]

The tail portion of the vehicle is an articulated structure composed of a four degree-of- freedom link assembly that acts upon a tuna-shaped flexible body. The tail is free flooded, and covered by an impermeable skin that prevents exchange of water across the envelope boundary.

The driven link assembly comprises three nearly equal length links and a caudal fin, all independently actuated by double-acting hydraulic cylinders. Hydraulic lines penetrating the aft end of the pressure hull connect the hydraulic power unit to the cylinders. At the aft end of each of the three links, a follower-rod assembly connects the links to the flexible exostructure.

The flexible exostructure converts the discrete movements of the link assembly to the smooth, fluid motions of a fish. The key elements of the exostructure are rigid buoyant foam “ribs” which are shaped like hollowed out tuna “steaks” and are connected to one another by two longitudinal flexible splines. The splines produce smooth curvature along the tail envelope simulating a mechanism containing a much greater number of links.

Table II: VCUUV system characteristics

Component	Description
Pressure hull	Carbon graphite/epoxy with aluminum mating surfaces
Computer and actutor control	PC104 486, DSP, hard drive
Sensors	3 accelerometers, 3 rate gyros, compass, pressure (depth), cylinder displacement and force, leak detectors, internal temperature
Actuators	Recirculating hydraulic system for tail linkage, motor for pectoral fins
Energy	Sealed lead acid batteries, 60 VDC, 800 W-hr
Communications	Ethernet through umbilical (when attached) status indicator lights

https://doi.org/10.1017/S0263574799002246 Published online by Cambridge University Press

The structure-fluid interface is a sub-dermal layer of overlapping scales which prevent circumferential folds between the ribs. The outermost layer consists of neoprene rubber that is bonded to nylon fabric on both sides. This "skin" prevents water movement across the boundary while maintaining an extremely smooth flexible surface which is nearly impermeable to water. At the end of the tail is the rigid caudal fin which is the primary propulsive actuator. The fin shape was determined by averaging direct measurement of a yellowfin tuna cast that we prepared and measurements made from photographs of freshly caught fish. The cross section was determined by sectioning the cast caudal fin in multiple locations.

As in real tunas, depth control of the VCUUV is provided by means of two pectoral fins. Real tunas (which are generally negatively buoyant) use their pectoral fins to dynamically control depth. At low speeds, the fins are fully splayed for maximum lift; as the speed increases, the fin sweepback angle is increased until the fins are fully adducted, effectively reducing the lifting area.

The VCUUV pectoral fins are positioned in the same location as real tuna pectoral fins: slightly forward of the center of gravity. Thus, the pectoral fins act as canards. Unlike actual tunas which can articulate their pectoral fins in pitch and sweep angle, the VCUUV pectoral fins only pitch, controlled by torquemotors located inside the pressure hull. For simplicity, the pectoral fin shapes are swept and tapered NACA 0015 sections roughly matching the chord and span of actual tuna fins. Because of the large metacentric height of the vehicle, pectoral fin lift allows depth control and correction of ballasting errors without inducing pitch or roll. Two rigid keel like fins (dorsal and anal) attached just aft of the hull/tail interface are included for stability. These fins were constructed in the same manner as the caudal fin.

Twenty days of testing and approximately 100 autonomous experiments have been completed with the VCUUV beginning with the vehicle's first swim in April, 1998 in a swimming pool. Preliminary trials were completed at the University of New Hampshire Ocean Engineering Laboratory in a 60×40 feet by 20 feet deep freshwater tank. Autonomous swimming and turning were achieved early in the experiments with no physical or electrical connections to the ground station. Figure 16 shows the deployment of the vehicle and autonomous swimming and turning experiments during the tank trials.

In the summer and fall of 1998, the VCUUV was tested in two local freshwater ponds in Hopkinton State Park (Hopkinton, MA) and Nickerson State Park (Brewster, MA). The VCUUV pond experiments took advantage of the larger bodies of water by swimming longer and more aggressive missions. Experiments in heading control were conducted yielding straight, circular, square, and zig-zag trajectories by closing control loops on the magnetic compass measurement. Swimming kinematic parameters were varied for straight swimming and maneuvering to identify the key parameters and how they affect swimming performance.

Field trial results have demonstrated the excellent maneuverability of the VCUUV as compared to conventional underwater vehicles. The VCUUV achieved a sustained circular trajectory of one body length in diameter and very high turn rates in aggressive maneuvers. Turning rates up to 75 degrees per second were obtained in a hard turn at 1.2 m/s which resulted in the vehicle coming to a full stop. in a zigzag trajectory, the VCUUV was able to

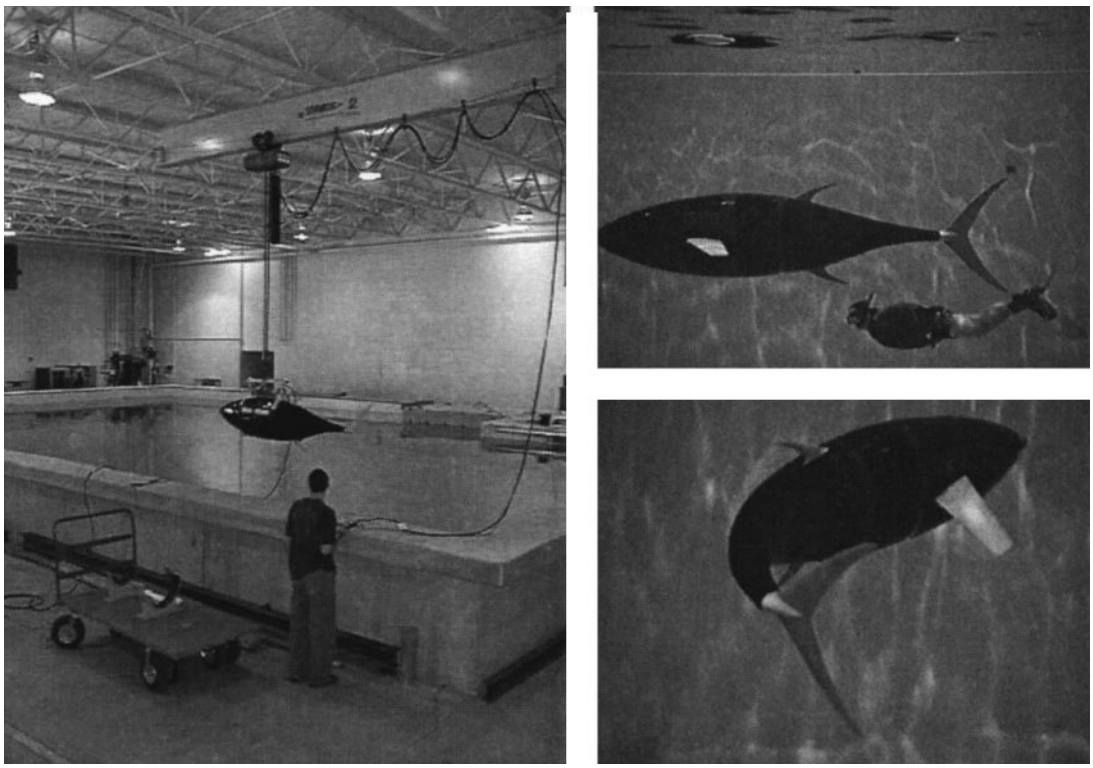


Fig. 16. VCUUV deployment during tank trials and autonomous swimming and maneuvering.

https://doi.org/10.1017/S0263574799002246 Published online by Cambridge University Press

maintain steady forward speed while making aggressive course changes at 30 degrees per second. This level of maneuverability enables rapid response obstacle avoidance and operation in cluttered environments.

The successful demonstration of the VCUUV has demonstrated a novel propulsion and maneuvering paradigm which can compete with conventional propulsors energetically while outperforming them by an order of magnitude in maneuverability. This revolutionary mobility is the key to achieving success in the challenging missions of underwater vehicles now and in the future.

5. CONCLUSIONS

Examples of vehicles for air, land, and water operations developed in the Intelligent Unmanned Vehicle Center have been highlighted. Further details on the individual systems are available in the references. Further capabilities and miniaturization of unmanned systems are enabled through fast paced advances in MEMS sensors and MCM packaging. Future envisioned systems expand the operational envelope for autonomous capabilities.

References

1. C. Sanders, P. DeBitetto, E. Feron, H.F. Vuong and N. Leveson, "Hierarchical control of small autonomous helicopter", *Proc. of the 37th IEEE Conference on Decision and Control*, Tampa, FL (December, 1998) pp. 3629–3634.
2. E. Johnson, P. DeBitetto, C. Trott and M. Bosse, "The 1996 MIT/Boston University/Draper Laboratory Autonomous Helicopter System", *Proc. of the AIAA/IEEE Digital Avionics System Conference* (1996) pp. 381–386.
3. W. Kaliardos. "Sensors for autonomous navigation and hazard avoidance on a planetary micro-rover" *Proc. of SPIE 2220*, Orlando, FL (April 4–8, 1994) pp. 59–68.
4. E. Malafeew, "Planning and control in a semi-autonomous planetary micro-rover", *Proc. of SPIE 2221*, Orlando, FL, (April 4–8, 1994) pp. 136–147.
5. B. Koontz, C. Tung, E. Wilson and D. Kang, "SMART: SMall Autonomous Robotic Technician", *Proc. of the Symposium on Technology and the Mine Problem*, Naval Postgraduate School, Monterey, CA (Nov. 18–21, 1996) pp. 511–522.
6. J. Thele and D. Kang, "Micro-rover operator station", *Proc. of the SAE International Environmental Systems Conference*, paper # 981696, Danvers, MA (July 13–16, 1998).
7. T. Chow, S. Steiner, W. Kaliardos and D. Kang, "Companion: An Autonomous Ground Vehicle", *Proc. of AIAA Robotics Technology Forum*, pp. 3.1–3.6, Madison, WI (August, 1996) pp. 3.1–3.6.
8. J.M. Anderson and P.A. Kerrebrock, "The vorticity control unmanned undersea vehicle (VCUUV) – an autonomous vehicle employing fish swimming propulsion and maneuvering", *Proc. of the Autonomous Undersea System Institute 10th International Symposium on Unmanned Untethered Submersible Technology*, Durham, NH (September 7–10, 1997) pp. 189–195.

https://doi.org/10.1017/S0263574799002246 Published online by Cambridge University Press